

## Isospin symmetry of $T_z = \pm 3/2 \rightarrow \pm 1/2$ Gamow-Teller transitions in $A=41$ nuclei

Y. Fujita,<sup>1,\*</sup> Y. Shimbara,<sup>1,†</sup> T. Adachi,<sup>1</sup> G. P. A. Berg,<sup>2,3</sup> B. A. Brown,<sup>4</sup> H. Fujita,<sup>1,‡</sup> K. Hatanaka,<sup>2</sup> J. Kamiya,<sup>2,§</sup> K. Nakanishi,<sup>2</sup> Y. Sakemi,<sup>2</sup> S. Sasaki,<sup>5</sup> Y. Shimizu,<sup>5</sup> Y. Tameshige,<sup>2</sup> M. Uchida,<sup>6</sup> T. Wakasa,<sup>2,||</sup> and M. Yosoi<sup>6</sup>

<sup>1</sup>Department of Physics, Osaka University, Toyonaka, Osaka 560-0043, Japan

<sup>2</sup>Research Center for Nuclear Physics, Osaka University, Ibaraki, Osaka 567-0047, Japan

<sup>3</sup>KVI, Zernikelaan 25, 9747 AA Groningen, The Netherlands

<sup>4</sup>NSCL and Department of Physics and Astronomy, Michigan State University, East Lansing, Michigan 48824, USA

<sup>5</sup>Shizuoka Institute of Technology, Fukuroi, Shizuoka 437-8555, Japan

<sup>6</sup>Department of Physics, Kyoto University, Kyoto 606-8502, Japan

(Received 31 July 2004; published 12 November 2004)

Under the assumption that isospin  $T$  is a good quantum number, isobaric analog states and various analogous transitions are expected in isobars with mass number  $A$ . The strengths of  $T_z = \pm 3/2 \rightarrow \pm 1/2$  analogous Gamow-Teller (GT) transitions and analogous  $M1$  transitions within the  $A=41$  isobar quartet are compared in detail. The  $T_z = +3/2 \rightarrow +1/2$  GT transitions from the  $J^\pi = 3/2^+$  ground state of  $^{41}\text{K}$  leading to excited  $J^\pi = 1/2^+$ ,  $3/2^+$ , and  $5/2^+$  states in  $^{41}\text{Ca}$  were measured using the  $(^3\text{He}, t)$  charge-exchange reaction. With a high energy resolution of 35 keV, many fragmented states were observed, and the GT strength distribution was determined up to 10 MeV excitation energy ( $E_x$ ). The main part of the strength was concentrated in the  $E_x = 4-6$  MeV region. A shell-model calculation could reproduce the concentration, but not so well details of the strength distribution. The obtained distribution was further compared with two results of  $^{41}\text{Ti}$   $\beta$  decay studying the analogous  $T_z = -3/2 \rightarrow -1/2$  GT strengths. They reported contradicting distributions. One-to-one correspondences of analogous transitions and analog states were assigned up to  $E_x = 6$  MeV in the comparison with one of these  $^{41}\text{Ti}$   $\beta$ -decay results. Combining the spectroscopic information of the analog states in  $^{41}\text{Ca}$  and  $^{41}\text{Sc}$ , the most probable  $J^\pi$  values were deduced for each pair of analog states. It was found that  $5/2^+$  states carry the main part of the observed GT strength, while much less GT strength was carried by  $1/2^+$  and  $3/2^+$  states. The gross features of the GT strength distributions for each  $J$  were similar for the isospin analogous  $T_z = \pm 3/2 \rightarrow \pm 1/2$  transitions, but the details were somewhat different. From the difference of the distributions, isospin-asymmetry matrix elements of  $\approx 8$  keV were deduced. The Coulomb displacement energy, which is sensitive to the configuration of states, showed a sudden increase of about 50 keV at the excitation energy of 3.8 MeV. The strengths of several  $M1$  transitions to the IAS in  $^{41}\text{Ca}$  were compared with the strengths of analogous GT transitions. It was found that ratios of the  $M1$  and GT transition strengths were similar, suggesting that the contributions of the  $\ell\tau$  term in  $M1$  transitions are small.

DOI: 10.1103/PhysRevC.70.054311

PACS number(s): 25.55.Kr, 21.10.Hw, 21.60.Cs, 27.40.+z

### I. INTRODUCTION

Isospin is a good quantum number under the assumption that the nuclear interaction is charge symmetric and that the effect of the electromagnetic interaction is relatively small. As such, an analogous structure is expected for the same mass  $A$  nuclei with different  $T_z$  (isobars), where  $T_z = [(N - Z)/2]$  is the  $z$  component of the isospin  $T$  (see, e.g., Refs. [1,2]). The corresponding states in different  $T_z$  nuclei are called isobaric analog states (or simply analog states). Transitions connecting various combinations of analog states are analogous. Such “analogous transitions” should have corre-

sponding energies and strengths. Properties and isospin symmetry of analogous transitions in isobars have been discussed extensively in Refs. [1,3].

Gamow-Teller (GT) transitions, caused purely by the  $\sigma\tau$ -type operator, are well suited for the study of analog states and properties of analogous transitions, because they can be studied in both  $\beta$  decay and hadron charge-exchange (CE) reactions. The GT transitions are characterized by  $\Delta L = 0$ ,  $\Delta S = 1$ , and  $\Delta T_z = \pm 1$ , where  $L$  and  $S$  are the orbital and spin quantum numbers. An important physical quantity for understanding the nuclear structure is the reduced GT transition strength  $B(\text{GT})$ . The  $B(\text{GT})$  values are usually obtained from studies of GT  $\beta$  decay. In addition, CE reactions, such as  $(p, n)$  or  $(^3\text{He}, t)$ , performed at intermediate energies ( $>100$  MeV/nucleon) can be used as a means to map the GT strengths over a wide range of excitation energy ( $E_x$ ) [4,5]. For this purpose, one relies upon the approximate proportionality between the reaction cross sections measured at the scattering angle  $\Theta = 0^\circ$  and their  $B(\text{GT})$  values [6].

The simplest analogous GT transitions are expected for the odd-mass mirror nuclei with  $T_z = \pm 1/2$ . By comparing the GT transitions from the ground states of  $T_z = -1/2$  and

\*Electronic address: fujita@rcnp.osaka-u.ac.jp

†Present address: Research Center for Nuclear Physics, Osaka University, Ibaraki, Osaka 567-0047, Japan.

‡Present address: iThemba LABS, P.O. Box 722, Somerset West 7129, South Africa.

§Present address: JAERI, Tokai, Ibaraki 319-1195, Japan.

||Present address: Department of Physics, Kyushu University, Higashi, Fukuoka 812-8581, Japan.

+1/2 nuclei to excited states of  $T_z = +1/2$  and  $-1/2$  nuclei studied in  $\beta$  decays and  $(p, n)$ -type CE reactions, respectively, the symmetry of analogous transitions and analog states, and thus the isospin symmetry of isobars, has been discussed in the low-lying region of various  $sd$ -shell nuclei [6–9]. Similarly, the symmetric nature of  $T_z = \pm 1$  to  $T_z = 0$  GT transitions has been examined for a few systems of light  $sd$ -shell nuclei, such as the  $A=26$  nuclei system ( $^{26}\text{Mg}$ ,  $^{26}\text{Al}$ , and  $^{26}\text{Si}$ ) [10,11] or the  $A=38$  system ( $^{38}\text{Ar}$ ,  $^{38}\text{K}$ , and  $^{38}\text{Ca}$ ) [12] by comparing  $(p, n)$  or  $(^3\text{He}, t)$  CE reactions and  $\beta$ -decay studies. A good correspondence of  $B(\text{GT})$  values with a difference of less than 5% was observed for the four strong  $T_z = \pm 1 \rightarrow T_z = 0$  GT transitions in the  $A=26$  system [11], and thus a good isospin symmetry was found. However, such a comparison was possible only for the low-lying states up to  $E_x \approx 3$  MeV due to the low  $Q_{\text{EC}}$  values of the relevant  $\beta$  decays [13]. An extension of the study to  $fp$ -shell nuclei with higher  $Q_{\text{EC}}$  values was discussed [14].

The symmetry of systems with larger isospin  $T$  is more challenging. The  $T_z = -T$  nuclei, unlike stable  $T_z = T$  nuclei, are usually far away from the  $\beta$ -stability line, and it is expected that the “isospin-asymmetric features,” if any, are observed better. The isospin structure and analogous transitions of the so-called “ $T=3/2$  system,” after subtracting the Coulomb displacement energy, are schematically shown in Fig. 1. The isobaric analog states of the  $T=3/2$  ground states of the  $T_z = \pm 3/2$  nuclei are called the IAS in the  $T_z = \pm 1/2$  nuclei. There are several stable  $T_z = 3/2$  nuclei in the  $sd$ - and  $fp$ -shell regions. The GT transitions from the ground state (g.s.) of a  $T_z = +3/2$  nucleus to  $\Delta J^\pi = 1^+$  states (GT states) in a  $T_z = +1/2$  nucleus can be studied via CE reactions, such as  $(p, n)$  or  $(^3\text{He}, t)$ . The measurements of the corresponding  $T_z = -3/2$  to  $T_z = -1/2$  transitions in  $\beta$  decays have become more accurate in recent years with the technical development of producing a larger number of unstable nuclei with greater purity. It should be noted that these  $\beta$  decays have relatively high  $Q_{\text{EC}}$  values of more than 10 MeV. Therefore, it is expected that not only the transitions to the low-lying states, but also the main part of the GT transition strengths can be studied in these  $\beta$ -decay measurements.

Among the candidates for the  $T_z = \pm 3/2 \rightarrow \pm 1/2$  comparison, we find that analogous transitions in the  $A=41$  system—i.e.,  $^{41}\text{K}$  ( $T_z = +3/2$ ) to  $^{41}\text{Ca}$  ( $T_z = +1/2$ ) and  $^{41}\text{Ti}$  ( $T_z = -3/2$ ) to  $^{41}\text{Sc}$  ( $T_z = -1/2$ )—are well suited for an accurate study of the analogous GT transitions and also the isospin-symmetry structure of isobars. The former can be studied by a CE reaction on a stable  $^{41}\text{K}$  target and the latter in the  $\beta$  decay of  $^{41}\text{Ti}$ . Owing to the high  $Q_{\text{EC}}$  value of 12.93 MeV in the  $^{41}\text{Ti}$   $\beta$  decay [15], the  $B(\text{GT})$  values have been reported for  $^{41}\text{Sc}$  up to about 8 MeV by several groups [16–19].

In this paper, we report the GT strengths of the  $T_z = +3/2 \rightarrow +1/2$  GT transitions up to  $E_x = 10.5$  MeV deduced from a measurement of the  $^{41}\text{K}(^3\text{He}, t)^{41}\text{Ca}$  reaction at  $0^\circ$ . These  $B(\text{GT})$  values are compared with those of the isospin-symmetric  $T_z = -3/2 \rightarrow -1/2$  GT transitions from  $^{41}\text{Ti}$   $\beta$  decay. In order to make a reliable comparison, high energy resolution is important in the CE reaction. Good angular resolution is also important in order to obtain a well-defined  $0^\circ$  spectrum. In our  $^{41}\text{K}(^3\text{He}, t)$  measurement, a high energy

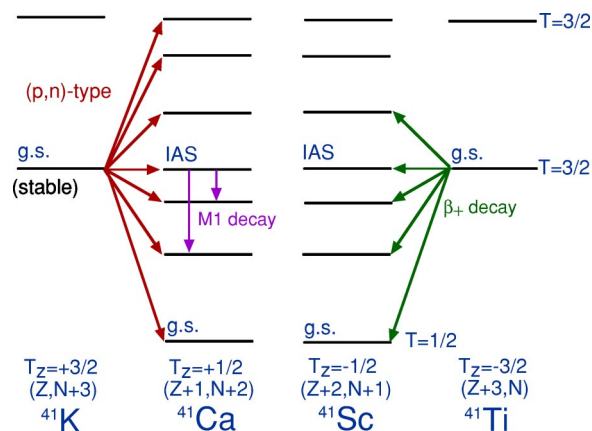


FIG. 1. (Color online) Schematic view of the isospin analog states and analogous transitions in the  $A=41$ ,  $T_z = \pm 3/2$  and  $\pm 1/2$  isobar system. The Coulomb displacement energies are removed so that the isospin symmetry of the states and transitions become clearer. The type of the reaction or decay is shown along the arrow indicating the transition.

resolution of 35 keV and a good angular resolution were realized even at an intermediate incident energy of 420 MeV (140 MeV/nucleon) by using a magnetic spectrometer in combination with beam matching techniques [20].

## II. EXPERIMENT

The GT states are predominantly excited in CE reactions at intermediate energies ( $\geq 100$  MeV/nucleon) and at forward scattering angles including  $0^\circ$ . This is because of the  $L=0$  nature of GT states and the dominance of the  $\sigma\tau$  part of the effective nuclear interaction [21]. The experiment was performed at the Research Center for Nuclear Physics (RCNP), Osaka, by using a 140 MeV/nucleon  $^3\text{He}$  beam from the  $K=400$  RCNP Ring Cyclotron and the QDD-type Grand Raiden spectrometer [22] placed at  $0^\circ$ . The beam was stopped in a Faraday cup inside the first dipole magnet. In a  $(^3\text{He}, t)$  experiment using a magnetic spectrometer, the measurement at  $0^\circ$  is relatively easy, because the magnetic rigidities of the  $^3\text{He}^{2+}$  beam and the singly charged outgoing tritons differ by about a factor of 2. However, for the analysis of intermediate-energy tritons, a large bending power is required for the spectrometer. This requirement makes the Grand Raiden spectrometer ideally suited for the present measurement. The large difference of atomic energy losses of  $^3\text{He}$  and tritons in a target foil can cause a large energy spread of the outgoing tritons, which deteriorates the spectral resolution. Therefore, a thin self-supporting foil is desirable as a target.

In order to produce a thin  $^{41}\text{K}$  self-supporting target, a thin foil of  $^{41}\text{K}_2\text{CO}_3$  supported by polyvinylalcohol (PVA) [23] was used. The enrichment of the  $^{41}\text{K}$  isotope was 99.2%. The total thickness of the target was approximately 1 mg/cm<sup>2</sup>. Therefore, this target is a mixture of  $^{41}\text{K}$ , carbon isotopes  $^{12}\text{C}$  and  $^{13}\text{C}$  with natural abundance 98.9% and 1.1%, respectively, and oxygen isotopes  $^{16}\text{O}$  and  $^{18}\text{O}$  with

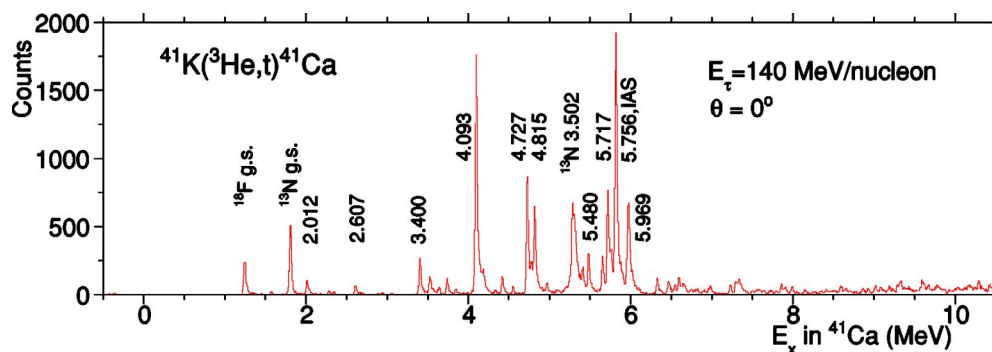


FIG. 2. (Color online) The  $^{41}\text{K}(^3\text{He},t)^{41}\text{Ca}$  spectrum at  $0^\circ$  with an angular range up to  $0.5^\circ$ . A high resolution of 35 keV has been achieved. The major GT states are indicated by their excitation energies. For other details, see text.

natural abundance 99.8% and 0.2%, respectively. The final nuclei after the  $(^3\text{He},t)$  charge-exchange reactions are  $^{41}\text{Ca}$ ,  $^{12}\text{N}$ ,  $^{13}\text{N}$ ,  $^{16}\text{F}$ , and  $^{18}\text{F}$ , respectively, and their reaction  $Q$  values are  $-0.42$ ,  $-17.36$ ,  $-2.24$ ,  $-15.44$ , and  $-1.67$  MeV. Owing to the large difference of  $Q$  values, states in  $^{41}\text{Ca}$  can be observed without being affected by the strongly excited states in  $^{12}\text{N}$  and  $^{16}\text{F}$ . Since the  $Q$  values of  $^{13}\text{C}$  and  $^{18}\text{O}$  nuclei are comparable with that of  $^{41}\text{Ca}$ , the ground and excited states of  $^{13}\text{N}$  and  $^{18}\text{F}$  are expected in the  $^{41}\text{Ca}$  spectrum. The separation and identification of these states and the states of  $^{41}\text{Ca}$  were possible owing to the high energy resolution of this experiment, as will be described below.

The outgoing tritons were momentum analyzed without using any acceptance-defining aperture of the spectrometer. A spectrum covering the angular range of  $\approx \pm 20$  mrad horizontally ( $x$ ) and  $\approx \pm 40$  mrad vertically ( $y$ ) was obtained. The tritons were detected at the focal plane with a multiwire drift-chamber system allowing track reconstruction for each ray [24]. The acceptance of the spectrometer was subdivided in the software analysis by using this track information.

An energy resolution far better than the energy spread of the beam was realized by applying the *dispersion matching* technique [25]. Using the new high-resolution “WS course” [26] for the beam transport and the “faint beam method” for the diagnosis of matching conditions [27,28], an unprecedented resolution of 35 keV [full width at half maximum (FWHM)] was achieved. This improved resolution allowed us to resolve states of  $^{41}\text{Ca}$  up to  $E_x = 10$  MeV, as shown in Fig. 2. As can be seen, all strongly excited states are concentrated in the energy region between 4 and 6 MeV. The g.s. of  $^{18}\text{F}$  and the g.s. and the 3.502 MeV state of  $^{13}\text{N}$  were identified by comparing this spectrum with the spectrum of a  $^{\text{nat}}\text{MgCO}_3 + \text{PVA}$  target measured under the same condition as the  $^{41}\text{K}_2\text{CO}_3 + \text{PVA}$  target. They are indicated in Fig. 2. The higher excited states of  $^{13}\text{N}$  were also identified in the spectrum, but the contributions from these states were very small in the region  $E_x < 10.5$  MeV. The possible contributions from the states of  $^{39}\text{Ca}$  originating from the  $^{39}\text{K}$  nuclei with 0.8% isotopic abundance in the target were examined by comparing with the spectrum from the  $^{39}\text{K}_2\text{CO}_3 + \text{PVA}$  target. The strongest g.s. of  $^{39}\text{Ca}$  is expected at  $\approx 6.1$  MeV in the spectrum shown in Fig. 2, but no noticeable contribution was observed.

In order to accurately determine the scattering angle  $\Theta$  near  $0^\circ$ , angle measurements in both the  $x$  direction ( $\theta$ ) and  $y$  direction ( $\phi$ ) are equally important, where  $\Theta$  is defined by  $\Theta = \sqrt{\theta^2 + \phi^2}$ . Good  $\theta$  and  $\phi$  resolutions were achieved by applying the *angular dispersion matching* technique [25] and the “overfocus mode” in the spectrometer [29], respectively. The angle calibration was performed by using a multihole aperture. It is estimated that the angle resolution was better than 8 mrad [29]. The “ $0^\circ$  spectrum” in Fig. 2 shows events for scattering angles  $\Theta \leq 0.5^\circ$ . As will be shown, all prominent states are of  $L=0$  nature.

Accurate  $E_x$  values with errors of about 1 keV are given in Ref. [30] for the  $\Delta J^\pi = 1^+$  GT states of  $^{41}\text{Ca}$  up to 6 MeV (see column 1 of Table I). However, we derived the  $E_x$  values independently. The  $^{26}\text{Mg}(^3\text{He},t)^{26}\text{Al}$  and  $^{24}\text{Mg}(^3\text{He},t)^{24}\text{Al}$  reactions have negative  $Q$  values of  $-4.02$  MeV and  $-13.90$  MeV, respectively. Accurate  $E_x$  values with errors of less than 1 keV are known for the  $1^+$  states of  $^{26}\text{Al}$  up to 7.9 MeV and for a few states in  $^{24}\text{Al}$  [7]. The  $^{16}\text{O}(^3\text{He},t)^{16}\text{F}$  reaction has a large negative  $Q$  value of  $-15.44$  MeV, and sharp  $1^+$  states are known up to 4.65 MeV [31]. On the other hand, the  $^{13}\text{C}(^3\text{He},t)^{13}\text{N}$  and  $^{18}\text{O}(^3\text{He},t)^{18}\text{F}$  reactions have small negative  $Q$  values of  $-2.24$  MeV and  $-1.67$  MeV, respectively. States from all of these reactions were observed in the spectrum using a  $^{\text{nat}}\text{MgCO}_3 + \text{PVA}$  target [23] measured under the same condition as with the  $^{41}\text{K}_2\text{CO}_3 + \text{PVA}$  target. The  $E_x$  values of the states in the  $^{41}\text{K}(^3\text{He},t)$  spectrum were determined with the help of kinematic calculations. Owing to the large variety of  $Q$  values of the states used in the calibration, all  $E_x$  values of  $^{41}\text{Ca}$  states shown in column 3 of Tables I and II could be determined by interpolation. The present values agree with the literature values for most states up to  $E_x = 6$  MeV within 3 keV. The estimated errors are 5 keV for the states up to 8 MeV and 7 keV for higher excited states, unless indicated otherwise.

The yields of individual peaks were derived by applying a peak fitting program using the peak shape of the well separated  $^{39}\text{Ca}$  g.s. observed in the  $^{39}\text{K}(^3\text{He},t)$  measurement performed under the same condition as the  $^{41}\text{K}$  measurement. No obvious broadening of the width of  $^{41}\text{Ca}$  states was observed even for states above the proton separation energy  $S_p$  of 6.3 MeV.

TABLE I. States observed in the  $^{41}\text{K}(^3\text{He},t)^{41}\text{Ca}$  reaction below 7 MeV excitation energy and the corresponding GT transition strengths  $B(\text{GT})$ . For details of the derivation and the errors of  $B(\text{GT})$  values, see text.

Evaluated values <sup>a</sup>		$(^3\text{He}, t)^b$		
$E_x$ (MeV)	$2J^\pi; 2T$	$E_x$ (MeV)	$L$	$B(\text{GT})$
2.010	3 <sup>+</sup>	2.012	0	0.031(3)
2.606	5 <sup>+</sup>	2.607	0	0.020(3)
2.671	1 <sup>+</sup>	2.676	(0)	0.003(1)
2.884	7 <sup>+</sup>	2.884	$\geq 1$	
3.050	3 <sup>+</sup>	3.050	0	0.004(1)
3.400	1 <sup>+</sup>	3.400	0	0.067(6)
3.527	3 <sup>+</sup>	3.526	0	0.034(4)
3.740	(3,5) <sup>+</sup>	3.737	0	0.030(3)
3.846	1 <sup>+</sup>	3.845	0	0.012(2)
4.097	5 <sup>+</sup>	4.093	0	0.446(33)
4.184	(3,5)	4.182	0	0.034(4)
4.328	(3-13) <sup>(+)</sup>	4.330	$\geq 1$	
4.415	3 <sup>+</sup>	4.419	0	0.033(4)
4.550		4.550	0	0.014(2)
4.728	(3) <sup>+</sup>	4.727	0	0.220(17)
4.733	(5) <sup>+</sup>			
4.779	(3) <sup>+</sup>	4.777	0	0.033(5)
4.816	5 <sup>+</sup>	4.815	0	0.149(12)
		4.966	0	0.021(3)
5.095	3 <sup>+</sup>	5.097	0	0.011(2)
5.283	5 <sup>+</sup>	(5.28)		0.059(17)
5.411	5 <sup>+</sup>	5.406	(0)	0.045(10)
5.482	(3) <sup>+</sup>	5.480	0	0.079(7)
5.649	(5) <sup>-</sup>	5.652	0	0.067(6)
5.719	(5) <sup>-</sup>	5.717	0	0.190(15)
5.760	(5) <sup>+</sup>	5.756	0	0.051(6)
5.817	3 <sup>+</sup> ; 3 <sup>c</sup>	5.814	0	0.148(25) <sup>d</sup>
5.892	1 <sup>-</sup>	5.890	(0)	0.021(4)
5.976	(3,5) <sup>+</sup>	5.969	0	0.192(15)
		6.019	(0)	0.018(4)
6.325(5)	(5) <sup>+</sup>	6.326	0	0.031(3)
6.462(10)	(5-11) <sup>+</sup>	6.464	0	0.030(3)
		6.544	$\geq 1$	
		6.596	0	0.033(3)
6.647(2)	5 <sup>-</sup>	6.653	$\geq 1$	
6.738(7)	(5-11) <sup>+</sup>	6.744	$\geq 1$	
6.807(2)	(3) <sup>+</sup>	6.823	$\geq 1$	
6.822	1 <sup>+</sup>			
6.901(2)	5 <sup>+</sup>	6.904	0	0.007(1)
6.966(15)	3 <sup>+</sup> , 5 <sup>+</sup>	6.959	$\geq 1$	0.013(2)
		6.984	0	

<sup>a</sup>From Ref. [30].

<sup>b</sup>Present work.

<sup>c</sup>The IAS.

<sup>d</sup>For the details of the derivation, see text.

TABLE II. Continuation of Table I for the excitation energies between 7 and 10.5 MeV.

Evaluated values <sup>a</sup>		$(^3\text{He}, t)^b$		
$E_x$ (MeV)	$2J^\pi$	$E_x$ (MeV)	$L$	$B$ (GT)
		7.225	0	0.018(2)
7.296	5 <sup>-</sup>	7.296	0	0.024(3)
		7.332	0	0.026(3)
		7.37(2)	$\geq 1$	
		7.552	$\geq 1$	
		7.586	$\geq 1$	
		7.639	0	0.006(2)
		7.72(2)	$\geq 1$	
		7.792	(0)	0.006(2)
		7.854	0	0.018(3)
		7.901	$\geq 1$	
7.990(20)	1 <sup>+</sup> , 3 <sup>+</sup> , 5 <sup>+</sup>	7.986	0	0.010(4)
		8.046	0	0.002(1)
		8.144	0	0.008(2)
		8.272	( $\geq 1$ )	
		8.347	$\geq 1$	
8.402(2)	(5-11) <sup>+</sup>	8.406	(0)	0.009(2)
		8.468	$\geq 1$	
		8.515	$\geq 1$	
		8.587	0	0.016(3)
		8.653	$\geq 1$	
		8.702	$\geq 1$	
		8.861	0	0.011(3)
		8.926	0	0.009(2)
		9.013	0	0.016(3)
		9.081	$\geq 1$	
		9.183	$\geq 1$	
		9.230	(0)	0.006(2)
		9.324	( $\geq 1$ )	
		9.40(2)	$\geq 1$	
		9.590	(0)	0.019(4)
		9.616	$\geq 1$	
		9.669	0	0.014(3)
		9.771	$\geq 1$	
		9.862	(0)	0.004(2)
		9.928	$\geq 1$	
		10.03(2)	$\geq 1$	
		10.113	(0)	0.009(3)
		10.161	(0)	0.013(3)
		10.194	$\geq 1$	
		10.238	$\geq 1$	
		10.286	0	0.023(4)
		10.339	$\geq 1$	
		10.421	0	0.014(3)

<sup>a</sup>From Ref. [30].

<sup>b</sup>Present work.

### III. DATA ANALYSIS

#### A. Identification of $L=0$ Gamow-Teller states

In order to identify  $L=0$  GT states, yields were derived for all states in the spectra with angle cuts  $\Theta=0^\circ-0.5^\circ$  (see Fig. 2),  $0.5^\circ-1.0^\circ$ , and  $1.0^\circ-1.5^\circ$ . The angular distributions of GT states peak at  $0^\circ$ . The relative decrease of the yields of each state in these three cuts was compared with that of the 4.093 MeV state, the most strongly excited state known to have a pure GT nature. It was found that for most of the well-observed states below  $E_x=6$  MeV, the ratios of yields in the  $1.0^\circ-1.5^\circ$  and  $0^\circ-0.5^\circ$  angle cuts were similar to the ratio of the 4.093 MeV state within 20%, suggesting that they are all  $L=0$  states. On the other hand, a few very weakly excited states in this region and many weakly excited states above  $E_x=6$  MeV had ratios larger than 1.2 (typically 1.3–1.5), suggesting that these states have  $L \geq 1$ . They are indicated by the sign “ $\geq 1$ ” in column 4 of Tables I and II.

#### B. $B(\text{GT})$ evaluation from $({}^3\text{He}, t)$ data

It is known that in CE reactions at  $0^\circ$  the cross sections for GT transitions are approximately proportional to  $B(\text{GT})$  values [6,32,33]:

$$\frac{d\sigma_{\text{CE}}}{d\Omega}(0^\circ) \approx KN_{\sigma\tau}|J_{\sigma\tau}(0)|^2 B(\text{GT}) \quad (1)$$

$$= \hat{\sigma}_{\text{GT}} B(\text{GT}), \quad (2)$$

where  $J_{\sigma\tau}(0)$  is the volume integral of the effective interaction  $V_{\sigma\tau}$  at momentum transfer  $q=0$ ,  $K$  is the kinematic factor,  $N_{\sigma\tau}$  is a distortion factor, and  $\hat{\sigma}_{\text{GT}}$  is a unit cross section for the GT transition. For  $({}^3\text{He}, t)$  reactions, the approximate proportionality between the  $0^\circ$  cross sections and the GT transition strengths  $B(\text{GT})$  was shown for the  $B(\text{GT})$  values  $\geq 0.04$  from the studies of analogous GT transitions in  $A=27$ ,  $T=1/2$  mirror nuclei  ${}^{27}\text{Al}$  and  ${}^{27}\text{Si}$  [9] and  $A=26$  nuclei  ${}^{26}\text{Mg}$ ,  ${}^{26}\text{Al}$ , and  ${}^{26}\text{Si}$  [11]. Here we use a unit system that gives a value of  $B(\text{GT})=3$  for the  $\beta$  decay of the free neutron.

The product  $KN_{\sigma\tau}$  and therefore the unit cross section  $\hat{\sigma}_{\text{GT}}$  in Eq. (2) changes gradually as a function of mass number  $A$  as well as excitation energy [6]. In order to estimate the latter effect, a distorted-wave Born approximation (DWBA) calculation was performed by using the code DW81 [34], assuming a simple  $d_{5/2} \rightarrow d_{3/2}$  transition for the excited GT states. The optical potential parameters used were those determined for  ${}^{28}\text{Si}$  at an incident  ${}^3\text{He}$  energy of 150 MeV/nucleon [35]. For the outgoing triton channel, by following the arguments given in Ref. [36], the well depths were multiplied by a factor of 0.85 without changing the geometrical parameters of the optical potential. For the effective projectile-target interaction of the composite  ${}^3\text{He}$  particle, the form derived by Schaeffer [37] by applying a folding procedure was used. As the interaction strength  $V_{\sigma\tau}$  and the range parameter  $R$  at 140 MeV/nucleon, we used the values of 2.1 MeV and 1.415 fm, respectively [38]. The calculated  $0^\circ$  cross section decreases by about 5% as  $E_x$  in-

creases up to 10 MeV. This result was used to correct the peak intensity of each state.

In order to obtain  $B(\text{GT})$  values from Eq. (2), we have to determine the unit cross section  $\hat{\sigma}_{\text{GT}}$  or the “unit GT intensity” for the transitions to the states observed in the  ${}^{41}\text{K}({}^3\text{He}, t){}^{41}\text{Ca}$  spectrum at  $0^\circ$ , shown in Fig. 2. However, there is no transition whose  $B(\text{GT})$  value can be directly determined from a  $\beta$ -decay measurement. Therefore, we assume that the total sum of  $B(\text{GT})$  values in the analogous mirror transitions—i.e.,  $T_z = \pm 3/2 \rightarrow \pm 1/2$  GT transitions—observed in the  ${}^{41}\text{K}({}^3\text{He}, t)$  reaction and in the  ${}^{41}\text{Ti}$   $\beta$  decay are the same (see Fig. 1). From Fig. 2, we see that most of the prominent levels are concentrated in the  $E_x=4-6$  MeV region. As discussed, most of them have  $L=0$ . A similar concentration of GT strength was reported in the corresponding  $E_x=4-6.2$  MeV region of  ${}^{41}\text{Sc}$  by Honkanen *et al.* [18] in one of the  $\beta$ -decay studies of  ${}^{41}\text{Ti}$  (for details, see Sec. V A). In addition, the sum of the  $B(\text{GT})$  values of  $\Sigma B(\text{GT})=1.77(17)$  in this region of  ${}^{41}\text{Sc}$ , except the GT strength in the IAS, was in good agreement within errors with the sum  $\Sigma B(\text{GT})=1.60(15)$  reported in another  $\beta$ -decay study by Liu *et al.* [19]. Therefore, the unit GT intensity was obtained by assuming that the total intensity summed over all GT states in this region, after making a correction for excitation energy, corresponds to the  $B(\text{GT})$  value of 1.68(12), which is the average of the  $\Sigma B(\text{GT})$  values of the two  $\beta$ -decay studies.

The  $B(\text{GT})$  values for all excited states, except for the IAS, were calculated by using the same unit GT intensity from their peak intensities after making the excitation energy correction. The obtained  $B(\text{GT})$  values are listed in column 5 of Tables I and II, and they are also displayed in Fig. 3(a). The errors quoted for these  $B(\text{GT})$  values come from the statistical uncertainties of the experimental data and the ambiguities of  $B(\text{GT})$  values in the  $\beta$ -decay measurement. On the other hand, the error associated with the possible isospin asymmetry of the strength in the  $E_x=4-6$  MeV region, where the normalization of the  $B(\text{GT})$  strength was performed, is not included. Since the proportionality given by Eq. (2) is experimentally established only for transitions with  $B(\text{GT}) \geq 0.04$  [9], the uncertainty may be larger for weaker transitions.

The transition from the  $J^\pi=3/2^+$  g.s. of  ${}^{41}\text{K}$  to the IAS can contain both Fermi (caused by the  $\tau$  operator) and GT components. In order to extract the GT component in the IAS, we assume that the Fermi transition strength concentrates to this IAS and the strength is  $B(\text{F})=N-Z=3$ . In addition, we used the fact that the ratio of GT and Fermi unit cross sections, denoted by  $R^2$  in Ref. [6], is only weakly dependent on mass number  $A$  and can be deduced to be 8.7(7) for the  $A=41$  nuclei by an interpolation between the known  $R^2$  values of 6.6(4) and 10.5(5) for  $A=26$  [11] and  $A=58$  [14,39] nuclei, respectively. In this way, we estimated a  $B(\text{GT})$  value of 0.148(25) in the transition to the IAS as the most probable value. In Ref. [18], an isospin impurity of  $(10 \pm 8)\%$  is suggested for the IAS. It is calculated that this amount of isospin impurity would increase the  $B(\text{GT})$  value in the IAS by  $0.034 \pm 0.028$ .

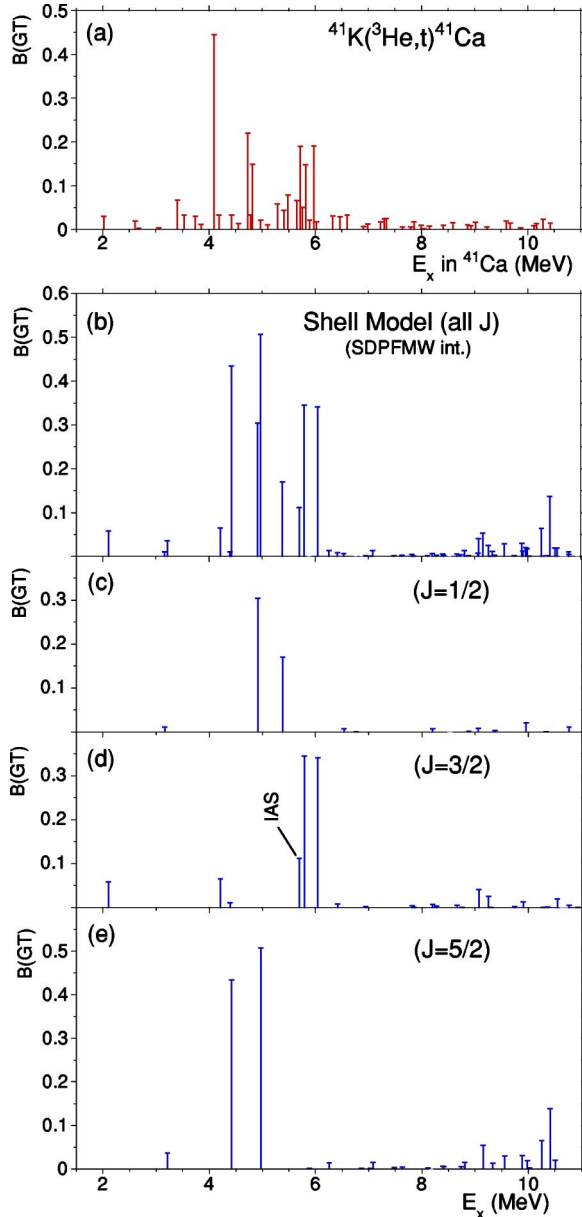


FIG. 3. (Color online) Experimental and shell-model  $B(\text{GT})$  distributions. (a)  $B(\text{GT})$  distribution from the present  $^{41}\text{K}(^3\text{He},t)^{41}\text{Ca}$  measurement. (b)  $B(\text{GT})$  distribution from a shell-model (SM) calculation for all allowed  $J$ .  $B(\text{GT})$  distribution from a SM calculation (c) for  $J=1/2$ , (d) for  $J=3/2$ , and (e) for  $J=5/2$ . Note the change in size of the panels.

#### IV. GAMOW-TELLER STATES AND $B(\text{GT})$ DISTRIBUTION

##### A. Experimental results

Since the g.s. of  $^{41}\text{K}$  has  $J^\pi=3/2^+$ , the  $L=0$ ,  $\Delta J^\pi=1^+$  GT transitions can reach either  $J^\pi=1/2^+$ ,  $3/2^+$ , or  $5/2^+$  states. For most states assigned to be  $L=0$  in the present analysis, corresponding states with either  $J^\pi=1/2^+$ ,  $3/2^+$ , or  $5/2^+$  can be found up to 7 MeV excitation energies in Ref. [30], as listed in Table I. Exceptions are the 4.550, 4.966, 5.652, 5.717, and 5.890 MeV states. For them either no  $J^\pi$  values or negative parity are assigned. No  $J^\pi$  values were given for the

4.550 MeV state, but possible  $J^\pi$  values of  $(1/2, 3/2, 5/2^+)$  are given for the probable analog state at 4.644 MeV in  $^{41}\text{Sc}$  (see Table III and the discussion of Sec. V A 2). The 4.966 MeV state is not known [30], but again its probable analog state with  $J^\pi$  values of  $1/2^+$  is found at 5.023 MeV. In Ref. [30] it is suggested that the 5.652 and 5.717 MeV states have negative parity. However, they are rather strongly excited in the  $0^\circ$  spectrum, and  $L=0$  is assigned in our analysis. In addition, possible analog states for these states with more or less corresponding strengths are observed at 5.774 and 5.840 MeV, respectively, in the  $^{41}\text{Ti}$   $\beta$ -decay measurement studying the isospin mirror GT transitions (see Table III). Therefore, we suggest that they are GT states with positive parity. We also suggest a positive parity for the 5.890 MeV state, although it is weaker. The  $J^\pi$  values of  $5/2^-$  are assigned to the 7.296 MeV state in Ref. [30]. Our analysis, however, shows  $L=0$  for the transition to this state, and a positive parity is therefore suggested.

As seen from Fig. 3(a), the main part of the GT strength is concentrated at  $E_x=4-6$  MeV, but it is very fragmented. Clustering of states is observed around 4.1, 4.75, 5.7, and 5.95 MeV.

##### B. $B(\text{GT})$ distribution from the shell model

The shell-model calculations for the  $A=41$  system were carried out in the  $sd$ - $fp$  model space. Relative to a closed  $sd$  shell for  $^{40}\text{Ca}$ , particles are in the  $fp$  shell and holes are in the  $sd$  shell. The model space was truncated to one-particle ( $1p$ ) for the low-lying  $T=1/2$  negative parity states and to two-particle one-hole ( $2p-1h$ ) for the excited  $T=1/2$  and  $3/2$  positive parity states. We used the SDPFMW Hamiltonian [40] that was deduced for this model space and truncation. The computer code OXBASH [41] was used in the calculation. In Fig. 3, the experimentally extracted  $B(\text{GT})$  values and the shell-model values are compared for excitation energies up to 10 MeV.

The results of shell-model calculation include the average renormalization factor (quenching factor) of 0.6 [13] for the  $B(\text{GT})$  values. By comparing Figs. 3(a) and 3(b), we see that the calculated and experimental  $B(\text{GT})$  distributions are generally in agreement. The observed concentration of the GT strength at  $E_x=4-6$  MeV and the fragmented and weakly excited strengths above 6 MeV are well reproduced by the calculation. The calculated total  $B(\text{GT})$  strength up to 6.5 MeV, where the main part of the strength is concentrated, is 2.43, which is in agreement with the corresponding experimental value of 2.12 within 15%. However, the observed fragmentation of the strength in the 4–6 MeV region was not reproduced. The calculated GT strength is concentrated in fewer states.

The calculation predicts that all  $T=3/2$  GT states, except for the IAS, are above  $E_x=7.5$  MeV. In addition, all of them have very small  $B(\text{GT})$  values. Therefore, it is suggested that most of the GT strength is in the transitions to the  $T=1/2$  states. In a naive picture, the structure of  $^{41}\text{K}$  is described by the  $^{40}\text{Ca}$  core plus two neutrons in the  $f_{7/2}$  shell and one proton hole in the  $d_{3/2}$  shell. The much weaker  $T=3/2$  strength compared to the  $T=1/2$  strength can be understood

TABLE III. Comparison of  $T_z = +3/2 \rightarrow +1/2$  and  $T_z = -3/2 \rightarrow -1/2$  analogous GT transitions observed in the  $^{41}\text{K}(^3\text{He}, t)^{41}\text{Ca}$  reaction and the  $\beta$  decay of  $^{41}\text{Ti}$  to  $^{41}\text{Sc}$ , respectively. The comparison is for the transitions to the states below 6.2 MeV, where the main part of the strength is concentrated.

$^{41}\text{K}(^3\text{He}, t)^{41}\text{Ca}^a$			$^{41}\text{Ti}$ $\beta$ decay to $^{41}\text{Sc}^b$			Deduced values		
$E_x$ (MeV)	$2J^\pi; 2T$	$B(\text{GT})$	$E_x$ (MeV)	$2J^\pi; 2T$	$B(\text{GT})$	$2J^{\pi d}$	$\Delta E_x$ (keV)	
2.012	3 <sup>+</sup>	0.031(3)	2.096	3 <sup>+</sup>	0.036(7)	3 <sup>+</sup>	84	
2.607	5 <sup>+</sup>	0.020(3)	2.667	5 <sup>+</sup>	0.067(13)	5 <sup>+</sup>	60	
2.676	1 <sup>+</sup>	0.003(1)	2.719	1 <sup>+</sup>	0.010(3)	1 <sup>+</sup>	43	
3.050	3 <sup>+</sup>	0.004(1)				3 <sup>+</sup>		
3.400	1 <sup>+</sup>	0.067(6)	3.411	1 <sup>+</sup>	0.061(7)	1 <sup>+</sup>	11	
3.526	3 <sup>+</sup>	0.034(4)	3.563	(1, 3, 5) <sup>+</sup>	0.031(6)	3 <sup>+</sup>	37	
3.737	(3, 5) <sup>+</sup>	0.030(3)	3.781	(5 <sup>+</sup> )	0.029(6)	5 <sup>+</sup>	44	
3.845	1 <sup>+</sup>	0.012(2)	3.951(14)	1 <sup>+</sup>	0.009(3)	1 <sup>+</sup>	106	
4.093	5 <sup>+</sup>	0.446(33)	4.245(4)	5 <sup>+</sup>	0.360(30)	5 <sup>+</sup>	152	
4.182	(3, 5)	0.034(4)	4.328(3)	5 <sup>+</sup>	0.016(4)	5 <sup>+</sup>	146	
4.419	3 <sup>+</sup>	0.033(4)	4.502(5)	3 <sup>+</sup>	0.014(4)	3 <sup>+</sup>	83	
4.550		0.014(2)	4.644(5)	1 <sup>-</sup>	0.015(4)		94	
4.727	(3) <sup>+</sup> , (5) <sup>+</sup>	0.220(17)	4.869(4)	5 <sup>+</sup>	0.015(20)	5 <sup>+</sup>	142	
4.777	(3) <sup>+</sup>	0.033(5)		4.777(5)	3 <sup>+</sup>	0.056(9)	3 <sup>+</sup>	0
4.815	5 <sup>+</sup>	0.149(12)		4.928(5)	(1, 3, 5) <sup>+</sup>	0.250(30)	5 <sup>+</sup>	113
4.966		0.021(3)	5.023(5)	1 <sup>+</sup>	0.031(8)	1 <sup>+</sup>	57	
5.097	3 <sup>+</sup>	0.011(2)	5.084(5)	3 <sup>+</sup>	0.031(8)	3 <sup>+</sup>	-13	
5.283	5 <sup>+</sup>	0.059(17)	5.375(4)	5 <sup>+</sup>	0.160(20)	5 <sup>+</sup>	92	
5.406	5 <sup>+</sup>	0.045(10)	5.493(5)	1 <sup>+</sup>	0.017(7)		87	
5.480	(3) <sup>+</sup>	0.079(7)	5.576(4)	3 <sup>+</sup> , 5 <sup>+</sup>	0.081(19)	3 <sup>+</sup>	96	
5.652	(5) <sup>-</sup>	0.067(6)	5.774(4)	(1, 3, 5) <sup>+</sup>	0.069(20)	5 <sup>+</sup>	122	
5.717	(5) <sup>-</sup>	0.190(15)		5.840(5)	3 <sup>+</sup> , 5 <sup>+</sup>	0.320(40)	5 <sup>+</sup>	123
5.756	(5) <sup>+</sup>	0.051(6)		5.886(12)	(1, 3, 5) <sup>+</sup>	0.069(19)	5 <sup>+</sup>	130
5.814	3 <sup>+</sup> ; 3 <sup>e</sup>	0.148(25)	5.939(4)	3 <sup>+</sup> ; 3 <sup>e</sup>	0.110 <sup>c</sup>	3 <sup>+</sup>	125	
5.890	1 <sup>-</sup>	0.021(4)	6.038(25)	(1, 3, 5) <sup>+</sup>	0.051(7)	1 <sup>+</sup>	148	
5.969	(3, 5) <sup>+</sup>	0.192(15)		6.083(20)	(1, 3, 5) <sup>+</sup>	0.060(8)		114
6.019		0.018(4)	6.133(20)	3 <sup>+</sup> , 5 <sup>+</sup>	0.053(7)		114	

<sup>a</sup>Present work.

<sup>b</sup>From Ref. [18].

<sup>c</sup>From the shell-model calculation; see Ref. [18].

<sup>d</sup>Suggested  $J^\pi$  values from the comparison.

<sup>e</sup>The IAS.

qualitatively with this picture in combination with the discussion given in Ref. [42] on the possible isospins for single-particle and single-hole configurations.

The shell-model calculation predicts an additional concentration of  $T=1/2$  strength around  $E_x=10$  MeV, which is not observed in the experiment. This predicted GT strength is probably spread over many  $5p$ - $3h$  states that are not in the model space, and thus the GT strength in this high energy region around 10 MeV may be blended into the continuum. A further comparison of strengths for each  $J$  value will be

made in Sec. V A 3. As will be discussed, the distributions for three different  $J$  states are not so well reproduced.

## V. COMPARISON OF ANALOGOUS TRANSITIONS

From Fig. 1, we see that the GT transitions studied in the  $\beta$  decay of the  $T_z = -3/2$  nucleus  $^{41}\text{Ti}$  to the  $T_z = -1/2$  nucleus  $^{41}\text{Sc}$  is analogous to those studied in the  $^{41}\text{K}(^3\text{He}, t)$  measurement. In addition, the  $M1$   $\gamma$  transitions from the IAS in  $^{41}\text{Ca}$  to lower excited states are also analogous. Our inter-

est is whether or not similarities of strengths are found for these different analogous transitions.

### A. Isospin-symmetric GT transitions

#### 1. GT transition strengths from $\beta$ -decay measurements

The GT strength distribution with  $T_z = +3/2 \rightarrow +1/2$  nature studied in the  $^{41}\text{K}(^3\text{He}, t)^{41}\text{Ca}$  reaction can be compared most directly with the result from the isospin-symmetric  $T_z = -3/2 \rightarrow -1/2$  transitions studied in the  $^{41}\text{Ti}$   $\beta$  decay. Owing to the high  $Q_{\text{EC}}$  value of this decay, the  $B(\text{GT})$  values can be studied for states in  $^{41}\text{Sc}$  with relatively high excitation energies. In Figs. 4(b) and 4(c), two  $B(\text{GT})$  distributions from the most recent  $^{41}\text{Ti}$   $\beta$ -decay measurements from Honkanen *et al.* [18] and from Liu *et al.* [19], respectively, are displayed. Because of the low  $S_p$  value of 1.09 MeV [30] in  $^{41}\text{Sc}$ , both distributions were derived from measurements of delayed protons. It was assumed that possible  $\gamma$  decays to the g.s. of  $^{41}\text{Sc}$  were not important, although such  $\gamma$  decays may have impact in some cases. In reality, the influence seems to be small, because similar  $B(\text{GT})$  values are observed in the  $T_z = \pm 3/2 \rightarrow \pm 1/2$  isospin mirror transitions to the lowest  $J^\pi = 3/2^+$  states (see Table III).

Both of these  $^{41}\text{Ti}$   $\beta$ -decay results show that the main part of the strength is found at excitation energies above 4 MeV. Similar clustering strengths can be seen at 4.25, 4.9, and 5.8 MeV, although the strengths are distributed somewhat differently in each cluster. The differences may be explained by the difference of the resolutions in measuring the energies of delayed protons. They are 30 keV in Ref. [18] [Fig. 4(b)] and 70–100 keV in Ref. [19] [Fig. 4(c)]. The total sums of  $B(\text{GT})$  values in the 4–6.2 MeV region, excluding the GT strength in the IAS, were 1.77(17) and 1.60(15) in Refs. [18,19], respectively, in agreement within the experimental errors. On the other hand, at higher excitations above 6.2 MeV, we see that these two  $\beta$ -decay results differ substantially.

#### 2. Corresponding GT states in $^{41}\text{Ca}$ and $^{41}\text{Sc}$

The GT strength distribution from our  $^{41}\text{K}(^3\text{He}, t)$  study is shown in Fig. 4(a) for the energy region where the  $\beta$ -decay results are available. It is clear that this distribution is quite similar to the one of Honkanen *et al.* [18] shown in Fig. 4(b) with respect to the gross structure. Furthermore, since the experimental resolutions in this  $\beta$ -decay measurement (30 keV) and the  $(^3\text{He}, t)$  reaction (35 keV) are both good and similar, we see a one-to-one correspondence of observed states and the GT transition strengths to them for the energy region below 6.2 MeV, where the main part of the GT strength is concentrated. By combining further the knowledge of  $J^\pi$  values of states in  $^{41}\text{Ca}$  and  $^{41}\text{Sc}$  evaluated in Ref. [30], correspondences of states are suggested in Table III, and details are discussed below.

In these two experiments detecting the isospin mirror transitions, we notice that the number of observed states with appreciable  $B(\text{GT})$  strength is identical in  $^{41}\text{Ca}$  and  $^{41}\text{Sc}$ , except for the very weak transition to the 3.050 MeV state observed in the  $(^3\text{He}, t)$  reaction. The residual interaction de-

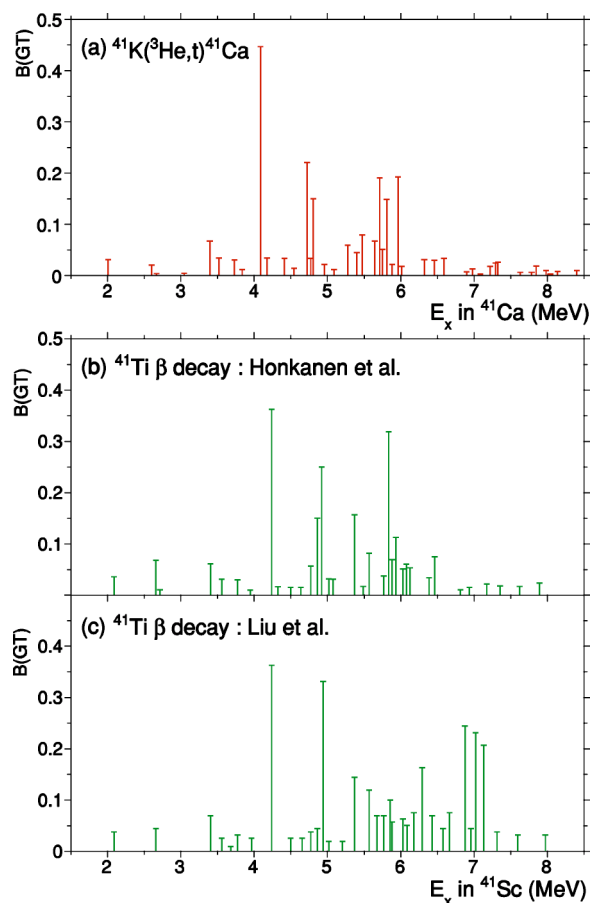


FIG. 4. (Color online) Experimental  $B(\text{GT})$  distributions from  $T_z = \pm 3/2 \rightarrow \pm 1/2$  isospin mirror transitions. (a)  $B(\text{GT})$  distribution from the present  $^{41}\text{K}(^3\text{He}, t)^{41}\text{Ca}$  reaction. (b)  $B(\text{GT})$  distribution from the  $^{41}\text{Ti} \rightarrow ^{41}\text{Sc}$   $\beta$  decay reported in Ref. [18]. (c)  $B(\text{GT})$  distribution from the  $^{41}\text{Ti} \rightarrow ^{41}\text{Sc}$   $\beta$  decay reported in Ref. [19].

pending on  $T_z$ —i.e., isospin-asymmetric interaction—can make the GT strength distribution somewhat different. However, since  $J$  is a good quantum number, the modification of the distribution is expected only among the same  $J$  states. Rather accurate excitation energies and  $J^\pi$  values have been evaluated for many of these states [30]. Therefore, the corresponding states can be assigned on the basis of excitation energies,  $J^\pi$  values, and the transition strengths from the  $(^3\text{He}, t)$  and  $\beta$ -decay measurements. A clear disagreement of  $J$  values is seen only for the corresponding states at 5.406 MeV in  $^{41}\text{Ca}$  and 5.493 MeV in  $^{41}\text{Sc}$ . They are given  $J^\pi$  values of  $5/2^+$  and  $1/2^+$ , respectively, in Ref. [30].

Since the number of observed states are practically the same, one may think that the corresponding states can be assigned by the ordering of the excitation energies, if we believe in the isospin symmetry. However, there are several clusters of states, and it is difficult to identify the corresponding states from only the sequence of excitation energies and the consistency of the assigned  $J^\pi$  values that sometimes have ambiguities. Clusters are at 4.75, 5.7, and 5.95 MeV in  $^{41}\text{Ca}$  and also in  $^{41}\text{Sc}$  at the corresponding energies [see Figs. 4(a) and 4(b)]. Clustering states are indicated by parentheses

between columns 3 and 4 in Table III. For these states, the corresponding states should be assigned taking the similarities of transition strengths into account in addition to the consistency of the assigned  $J^\pi$  values. As a result, it is suggested that the 4.727 and 4.777 MeV states of the first cluster in  $^{41}\text{Ca}$  correspond to the 4.869 and 4.777 MeV states in  $^{41}\text{Sc}$ , respectively; i.e., the order of the excitation energy of the corresponding states is reversed. Such a reversed order was noticed only for these pairs (see Table III).

For the analog states, the correlation of  $B(\text{GT})$  values between analogous  $T_z = \pm 3/2 \rightarrow \pm 1/2$  transitions was examined. As we see in Fig. 5, points are distributed more or less along the  $45^\circ$  line, but they are rather scattered, especially for pairs of states with smaller  $B(\text{GT})$  values. As a result, we conclude that the gross symmetry of these isospin mirror transitions is rather well preserved, but the fine structures are somewhat different.

### 3. Strength distributions of $J=1/2$ , $3/2$ , and $5/2$ states

The  $J^\pi$  values of the states in  $^{41}\text{Ca}$  and  $^{41}\text{Sc}$  have been evaluated independently for each nucleus [30]. Since the correspondence between analogous GT transitions became apparent in the present analysis, the knowledge of the  $J^\pi$  values for a pair of analog GT states can now be combined. The most probable  $J^\pi$  values of each pair of states were deduced up to  $E_x = 6$  MeV, and they are given in column 7 of Table III. We see that the number of  $J^\pi = 5/2^+$  states is the largest, while the number of  $1/2^+$  states is smaller, suggesting a large contribution of the  $d_{5/2}$  hole. The  $B(\text{GT})$  distributions of transitions to  $J=1/2$ ,  $3/2$ , and  $5/2$  states are shown in Figs. 6 and 7 for nuclei  $^{41}\text{Ca}$  and  $^{41}\text{Sc}$ , respectively. In both figures, the main part of the GT strength is found in the  $5/2^+$  states. Among the  $3/2^+$  states, the largest GT strength was seen in the  $T=3/2$  IAS at 5.814 MeV. Therefore, in comparison among  $T=1/2$  states, the dominance of the GT strength in  $5/2^+$  states is even more prominent.

When these  $B(\text{GT})$  distributions with three different  $J$  values are compared to the corresponding shell-model results shown in Figs. 3(c)–3(e), we see notable disagreements. In

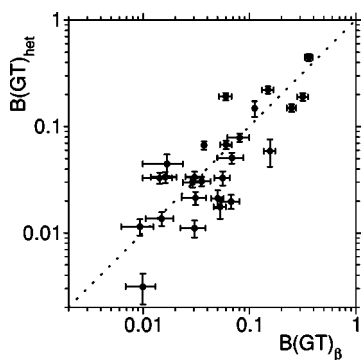


FIG. 5. A correlation of  $B(\text{GT})$  values between analogous  $T_z = \pm 3/2 \rightarrow \pm 1/2$  transitions. The  $-3/2 \rightarrow -1/2$   $B(\text{GT})_\beta$  values are from  $^{41}\text{Ti}$   $\beta$  decay [18] and the  $+3/2 \rightarrow +1/2$   $B(\text{GT})_{\text{het}}$  values are from the present  $^{41}\text{K}(^3\text{He}, t)$  measurement. Analog states with ideal correlation would follow the dashed line.

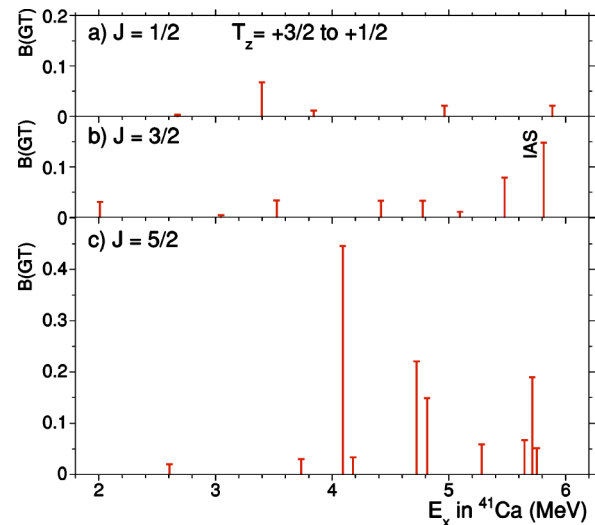


FIG. 6. (Color online) The  $T_z = +3/2 \rightarrow +1/2$   $B(\text{GT})$  distributions deduced from the  $^{41}\text{K}(^3\text{He}, t)$  measurement for the  $^{41}\text{Ca}$  states with (a)  $J^\pi = 1/2^+$ , (b)  $J^\pi = 3/2^+$ , and (c)  $J^\pi = 5/2^+$ .

the shell-model calculation, the  $J=1/2$  and  $3/2$  strengths are stronger than in the experiment, while the  $J=5/2$  strength is weaker. In addition, the fragmentation of the strength, especially that of the  $J=5/2$  strength in the  $E_x = 5-6$  MeV region is not well reproduced. The larger number of levels, and thus the higher level density, above about 5 MeV is probably due to the states of  $4p-3h$  levels that are not included in the model space truncation. These configurations cannot be reached directly from the  $2p-1h$ ,  $T=3/2$  g.s. However, above about 5 MeV, they could mix with the  $2p-1h$  doorway states and cause a spreading of the GT strength.

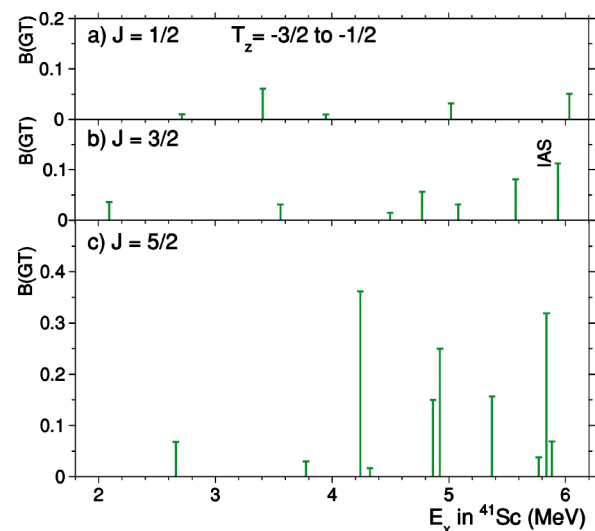


FIG. 7. (Color online) The  $T_z = -3/2 \rightarrow -1/2$   $B(\text{GT})$  distributions deduced from the  $^{41}\text{Ti}$   $\beta$ -decay measurement for the  $^{41}\text{Sc}$  states with (a)  $J^\pi = 1/2^+$ , (b)  $J^\pi = 3/2^+$ , and (c)  $J^\pi = 5/2^+$ .

#### 4. Estimation of the isospin-asymmetry matrix element

By comparing Figs. 6 and 7, we again notice that the gross features of these two  $B(\text{GT})$  distributions for the isospin mirror transitions are similar, but the details are somewhat different. One of the interesting features is that the strengths of two  $J=5/2$  states at about 4.8 MeV and 4.9 MeV in  $^{41}\text{Ca}$  and  $^{41}\text{Sc}$ , respectively, are almost reversed. It is natural to think that these reversed strengths in the  $T_z = \pm 3/2 \rightarrow \pm 1/2$  analog transitions are caused by the action of an interaction depending on  $T_z$ —i.e., an isospin-asymmetric interaction. For simplicity, let us think only of the mixture between these  $J=5/2$  doublet states. Then we can deduce that (A) the isospin-asymmetry matrix elements acting in these isospin mirror states have similar strengths but opposite signs and (B) without the isospin-asymmetry matrix elements the transition strengths to these doublet states are almost the same. We estimate the approximate values of isospin-asymmetry matrix elements on the basis of these assumptions.

The nuclear Hamiltonian is written as  $\mathcal{H} = \mathcal{H}_0 + \mathcal{H}_{1A}$ , where  $\mathcal{H}_0$  and  $\mathcal{H}_{1A}$  are the isospin-symmetry (conserving) term and isospin-asymmetry term, respectively. Two eigenstates of  $\mathcal{H}_0$  are denoted by  $\Phi_a$  and  $\Phi_b$ . Since the Hamiltonian  $\mathcal{H}_0$  is isospin symmetric, these wave functions are the same in both  $T_z = 1/2$  ( $^{41}\text{Ca}$ ) and  $T_z = -1/2$  ( $^{41}\text{Sc}$ ) nuclei. The excitation energies  $E_a$  and  $E_b$  of observed states are the eigenvalues of the total Hamiltonian  $\mathcal{H}$ . Let us think of wave functions  $\Psi_a$  and  $\Psi_b$  that satisfy

$$(\mathcal{H}_0 + \mathcal{H}_{1A})\Psi_a = E_a\Psi_a \quad (3)$$

and

$$(\mathcal{H}_0 + \mathcal{H}_{1A})\Psi_b = E_b\Psi_b, \quad (4)$$

respectively. The form of these equations is formally the same for  $T_z = \pm 1/2$  nuclei, but note here that the matrix elements in the isospin-asymmetry term  $\mathcal{H}_{1A}$  are different in the  $T_z = \pm 1/2$  nuclei [assumption (A)]. Therefore, the wave functions  $\Psi_a$  and  $\Psi_b$  are different in  $T_z = \pm 1/2$  nuclei.

We can formally write the states  $\Psi_a$  and  $\Psi_b$  in terms of linear combinations of the two states  $\Phi_a$  and  $\Phi_b$  as

$$\Psi_a = \alpha\Phi_a + \beta\Phi_b \quad (5)$$

and

$$\Psi_b = \beta\Phi_a - \alpha\Phi_b, \quad (6)$$

where  $\alpha^2 + \beta^2 = 1$ . Note again here that the coefficients  $\alpha$  and  $\beta$  are different in the  $T_z = \pm 1/2$  nuclei. Using these relationships, the matrix element of the off-diagonal matrix  $\mathcal{H}_{1A}$ —i.e., the isospin-asymmetry term—can be written as

$$\langle \Phi_a | \mathcal{H}_{1A} | \Phi_b \rangle = \alpha\beta(E_a - E_b). \quad (7)$$

Let us think of the GT transitions caused by the operator  $\mathcal{O} = \sigma\tau$  starting from the g.s.  $\Phi_0$  of  $T_z = \pm 3/2$  nuclei. For simplicity, we assume that the effect of isospin asymmetry in the g.s. is small. The GT transition strength  $B(\text{GT})$  is proportional to the squared value of the transition matrix element of  $\sigma\tau$  type, as will be discussed in Sec. V B. Therefore, the ratios of the  $B(\text{GT})$  values  $R^0$  and  $R^1$  for the transitions to the

two excited states before and after the mixing, respectively, can be expressed as

$$R^0 = \frac{B^0(\text{GT})_b}{B^0(\text{GT})_a} = \frac{|\langle \Phi_b | \mathcal{O} | \Phi_0 \rangle|^2}{|\langle \Phi_a | \mathcal{O} | \Phi_0 \rangle|^2} \quad (8)$$

and

$$R^1 = \frac{B^1(\text{GT})_b}{B^1(\text{GT})_a} = \frac{|\langle \Psi_b | \mathcal{O} | \Phi_0 \rangle|^2}{|\langle \Psi_a | \mathcal{O} | \Phi_0 \rangle|^2}, \quad (9)$$

where  $B^0(\text{GT})$  and  $B^1(\text{GT})$  are the  $B(\text{GT})$  values before the mixing of states and the observed  $B(\text{GT})$  values after the mixing of states, respectively. By putting Eqs. (5) and (6) into Eq. (9) and using  $R^0$ , the ratio  $R^1$  can be written as

$$R^1 = \frac{|\langle \beta\Phi_a - \alpha\Phi_b | \mathcal{O} | \Phi_0 \rangle|^2}{|\langle \alpha\Phi_a + \beta\Phi_b | \mathcal{O} | \Phi_0 \rangle|^2} \quad (10)$$

$$\simeq \frac{|\beta - \alpha\sqrt{R^0}|^2}{|\alpha + \beta\sqrt{R^0}|^2}. \quad (11)$$

The transformation from Eq. (10) to Eq. (11) is not exact when the associated phases are different in the matrix elements  $\langle \Phi_a | \mathcal{O} | \Phi_0 \rangle$  and  $\langle \Phi_b | \mathcal{O} | \Phi_0 \rangle$ .

There is no way to study the ratio  $R^0$  experimentally. However, according to assumption (B), we can put  $R^0 \approx 1$ ; i.e., the doublet states have almost equal  $B(\text{GT})$  values without the influence of  $\mathcal{H}_{1A}$ . Using the  $B(\text{GT})$  values listed in Table III, the values of  $R^1$  are obtained for the doublet states observed at 4.8 MeV in the ( $^3\text{He}, t$ ) study and also for the doublet states observed at 4.9 MeV in the  $\beta$ -decay study. A set of  $\alpha$  and  $\beta$  is obtained for each of these  $R^1$  values using Eq. (11) and the relationship  $\alpha^2 + \beta^2 = 1$ . The isospin-asymmetry matrix element is calculated by putting a set of  $\alpha$  and  $\beta$  and the difference of the excitation energies into Eq. (7). As a result, values of  $-8.3$  keV and  $7.5$  keV are obtained for the  $T_z = +3/2 \rightarrow +1/2$  and  $T_z = -3/2 \rightarrow -1/2$  transitions, respectively. The signs of them are opposite and the absolute values are nearly the same, which is consistent with assumption (A). It is interesting that relatively small isospin-asymmetry interactions of  $\approx 8$  keV can make the reversed transition strengths observed for the isospin mirror transitions to the doublet states with  $\Delta E \approx 70$  keV.

Isospin mixing was studied at a similar mass of  $A=37$  for a pair of  $J^\pi=3/2^+$  states. One of them was the  $T=3/2$  IAS in  $^{37}\text{K}$  at  $E_x=5.051$  MeV and the other was a  $T=1/2$  state lying 31 keV below. The relative proton widths of the two levels measured in a  $^{36}\text{Ar}(\vec{p}, p_0)$  resonance reaction implied an isospin-mixing matrix element of 4.8 keV [43]. In addition the analysis of the  $\beta^+$ -decay study from the g.s. of  $^{37}\text{Ca}$  to these two states suggested a value of 5.9 keV [43,44]. It is interesting that similar values are deduced for the isospin-asymmetry matrix element obtained here and the isospin-mixing matrix element.

#### 5. Difference of excitation energies in $^{41}\text{Ca}$ and $^{41}\text{Sc}$

The Coulomb displacement energy (CDE) is dependent on the configuration of each individual state [45,46]. In order

to study the CDE as a function of excitation energy, the difference of excitation energies,

$$\Delta E_x = E_x(^{41}\text{Sc}) - E_x(^{41}\text{Ca}), \quad (12)$$

was calculated for each pair of states. The  $\Delta E_x$  values are given in the last column of Table III. They are also plotted in Fig. 8 for different  $J^\pi$  states.

The  $\Delta E_x$  values of the  $J^\pi = 3/2^+$  states vary largely from  $-13$  to  $125$  keV [Fig. 8(b)], and the distribution is scattered as a function of  $E_x$ . The  $\Delta E_x$  distributions of the  $1/2^+$  and  $5/2^+$  states are less scattered. It is interesting that the minimum at  $E_x = 5.2$  MeV in the  $3/2^+$  distribution [Fig. 8(b)] is common with the local minimum in the distribution of the  $5/2^+$  states [Fig. 8(c)].

We see a clear discrete increase of  $\Delta E_x$  values at around  $E_x = 3.8$  MeV. In  $1/2^+$  and  $5/2^+$  distributions, a typical value of about  $50$  keV in the low-lying region changes suddenly up to more than  $100$  keV above  $4$  MeV excitation energies, where the main part of the strength appears. For the transitions in the low-lying region, the main configurations of  $d_{3/2} \rightarrow d_{3/2}$  and  $f_{7/2} \rightarrow f_{7/2}$  are expected in a naive single-particle model. On the other hand, at the higher excitation energies the main configurations of  $d_{5/2} \rightarrow d_{3/2}$  and  $f_{7/2} \rightarrow f_{5/2}$  are expected. The sudden increase of  $\Delta E_x$  values, corresponding to the sudden change of the CDE, suggests a change of the main configurations of the wave functions at around  $E_x = 3.8$  MeV.

### B. $M1$ $\gamma$ transitions in $^{41}\text{Ca}$

The  $M1$   $\gamma$  transitions from the IAS at  $E_x = 5.817$  MeV to low-lying states in  $^{41}\text{Ca}$  are analogous to the corresponding GT transitions observed in the  $^{41}\text{K}(^3\text{He}, t)$  reaction (see Fig. 1).

In order to compare  $M1$  transition strengths and  $B(\text{GT})$  strengths of analogous GT transitions, we have to examine the similarities and differences between these transitions. The GT operator has only an IV spin ( $\sigma\tau$ ) term. The GT transition strength  $B(\text{GT})$  reduced in isospin [47] is given by

$$B(\text{GT}) = \frac{1}{2J_i + 1} \frac{1}{2} \frac{C_{\text{GT}}^2}{2T_f + 1} [M_{\text{GT}}(\sigma\tau)]^2, \quad (13)$$

where  $C_{\text{GT}}$  is the isospin Clebsch-Gordan (CG) coefficient  $(T_i T_{zi} 1 \pm 1 | T_f T_{zf})$  with  $T_{zf} = T_{zi} \pm 1$ . The matrix element  $M_{\text{GT}}(\sigma\tau)$  denotes the GT transition matrix element of  $\sigma\tau$  type.

In addition to the IV spin ( $\sigma\tau$ ) term, the  $M1$  operator has an IV orbital ( $\ell\tau$ ) term and an IS term. Since the  $M1$  transitions of interest here are between the  $T = 3/2$  IAS and the  $T = 1/2$  GT states, only the IV terms can contribute. In which case, the  $M1$  transition strength  $B(M1)$  reduced in isospin [47] is given by

$$B(M1) = \frac{1}{2J_i + 1} \frac{3}{4\pi} \mu_N^2 \frac{C_{M1}^2}{2T_f + 1} \left[ g_\ell^{\text{IV}} M_{M1}(\ell\tau) + g_s^{\text{IV}} \frac{1}{2} M_{M1}(\sigma\tau) \right]^2, \quad (14)$$

where  $C_{M1}$  expresses the isospin CG coefficient

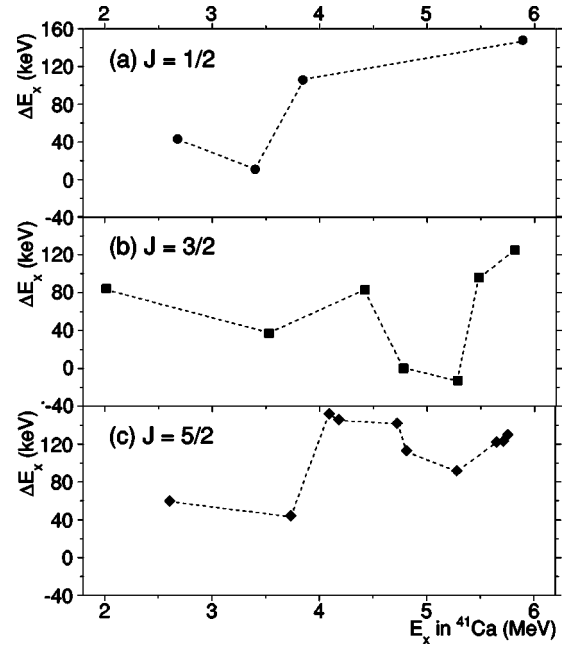


FIG. 8. The difference of excitation energies  $\Delta E_x$  for the corresponding states in  $^{41}\text{Sc}$  and  $^{41}\text{Ca}$ . The  $\Delta E_x$  values are plotted for pairs of states with (a)  $J = 1/2$ , (b)  $3/2$ , and (c)  $5/2$ . A clear sudden increase of  $\Delta E_x$  values is observed at  $E_x = 3.8$  MeV for the pairs of  $J = 1/2$  and  $5/2$  states. The dotted lines are drawn to guide the eye.

$(T_i T_{zi} 1 0 | T_f T_{zf})$  with  $T_{zf} = T_{zi}$ . The matrix elements  $M_{M1}(\sigma\tau)$  and  $M_{M1}(\ell\tau)$  denote the  $\sigma\tau$ -type and  $\ell\tau$ -type components of the  $M1$  transition matrix element, respectively. The IV combinations of spin and orbital  $g$  factors are expressed by  $g_s^{\text{IV}} = \frac{1}{2}(g_s^\pi - g_s^\nu)$  and  $g_\ell^{\text{IV}} = \frac{1}{2}(g_\ell^\pi - g_\ell^\nu)$ , respectively. Using the bare spin and orbital  $g$  factors of protons and neutrons—i.e.,  $g_s^\pi = 5.586$ ,  $g_s^\nu = -3.826$  and  $g_l^\pi = 1$ ,  $g_l^\nu = 0$ , we get  $g_s^{\text{IV}} = 4.706$  and  $g_\ell^{\text{IV}} = 0.5$ . Due to the large value of the coefficient  $g_s^{\text{IV}}$ , it is expected that the  $\sigma\tau$  term is usually larger than the  $\ell\tau$  term [48,49]. Therefore, corresponding strengths are expected for the analogous GT and  $M1$  transitions (for details, see, e.g., Ref. [47]).

The relative intensities  $I_\gamma$  and the energies  $E_\gamma$  of the  $\gamma$  transitions from the IAS to the states at  $E_x = 4.728$ ,  $4.097$ ,  $3.740$ ,  $3.400$ , and  $2.606$  MeV are given in Ref. [30] and are listed in column 4 of Table IV. Using these values, the transition strengths proportional to the  $M1$  transition strengths  $B(M1)$  can be deduced under the assumption that the  $E2$  and  $M1$  mixing ratios  $\delta$  are small for these transitions. The proportionality is given (see, e.g., Ref. [50]) by

$$B(M1) \propto \frac{1}{E_\gamma^3} I_\gamma. \quad (15)$$

The relative strengths of the  $B(M1)$  values for these five  $M1$  transitions are listed in column 5 of Table IV, and the relative strengths for the corresponding GT transitions are given in column 7, where the strongest  $M1$  and GT strengths to the  $4.097$  MeV are normalized to unity. As seen, the relative intensities of the analogous  $M1$  and GT transitions are in

TABLE IV. Comparison of analogous  $M1$  and  $GT$  transitions in  $A=41$  isobars. The  $\gamma$  transitions in  $^{41}\text{Ca}$  from the 5.817 MeV IAS to lower-lying states are analogous to the  $GT$  transitions to these states from the g.s. of  $^{41}\text{K}$ . Relative transition strengths are compared for these transitions assuming that these  $\gamma$  transitions are of pure  $M1$  nature.

States in $^{41}\text{Ca}$		$\gamma$ transitions in $^{41}\text{Ca}$			GT transitions to $^{41}\text{Ca}$	
$E_x$ (MeV) <sup>a</sup>	$2J^{\pi b}$	$E_\gamma$ (MeV)	Intensity <sup>c</sup>	$B(M1)$ ratio	$B(GT)$	$B(GT)$ ratio
2.606	$5^+$	3.211	23(4)	0.04(1)	0.020(3)	0.04(1)
3.400	$1^+$	2.417	30(4)	0.11(1)	0.067(6)	0.15(1)
3.740	$5^+$	2.077	15(9)	0.09(5)	0.030(3)	0.07(1)
4.097	$5^+$	1.720	100(8)	1.00(8)	0.446(33)	1.00(7)
4.728	$5^+$	1.089	21(4)	0.83(16)	0.220(17)	0.49(4)

<sup>a</sup>From Ref. [30].

<sup>b</sup>From the present analysis.

<sup>c</sup>Relative intensity from Ref. [30].

good agreement, except for the transitions to the 4.728 MeV state. From the similarity of corresponding  $GT$  and  $M1$  transitions strengths, it is suggested that the contributions of the  $\ell\tau$  term in the transitions are relatively small. It was found that such contributions of  $\ell\tau$  terms are very large for the deformed nuclei in the  $A=23-25$  mass region, where large enhancements or suppressions of  $M1$  strengths compared to the analogous  $GT$  transition strengths were observed [8,51,52].

## VI. SUMMARY

Isospin analogous  $GT$  and  $M1$  transitions were compared for  $A=41$  nuclei. Especially,  $T_z=\pm 3/2 \rightarrow \pm 1/2$  mirror  $GT$  transitions were compared and analyzed from various points of view.

The  $T_z=+3/2 \rightarrow +1/2$   $GT$  transitions were measured by using the  $^{41}\text{K}(^3\text{He},t)^{41}\text{Ca}$  reaction at  $0^\circ$  and at an intermediate incident energy of 140 MeV/nucleon. Thanks to the high energy resolution of 35 keV, states up to  $E_x=10$  MeV in  $^{41}\text{Ca}$  were clearly separated. This energy resolution of better than  $\Delta E/E=10^{-4}$  and also a good angle resolution of the scattering angle around  $0^\circ$  were achieved by the implementation of complete beam matching techniques between the magnetic spectrometer and the beamline. Highly fragmented discrete states were observed and the excitation energies of these states could be determined with an accuracy of less than 7 keV up to the excitation energy of 10 MeV. The  $B(GT)$  values in the  $(^3\text{He},t)$  reaction were calibrated by using  $B(GT)$  values derived in the  $GT$   $\beta$  decay from  $^{41}\text{Ti}$  to  $^{41}\text{Sc}$  by assuming mirror symmetry of the  $T_z=\pm 3/2 \rightarrow \pm 1/2$  transitions. A DWBA calculation was used to correct for the excitation energy dependence of the cross section. It was found that the main part of the  $GT$  strength is concentrated in the energy region between 3 and 6 MeV. The fragmentation of the  $GT$  strength was not so well reproduced by a shell-model calculation, suggesting more complicated structures of the  $A=41$  nuclei that extend over  $sd$ - and  $f$ -shell regions.

The mirror symmetric  $T_z=-3/2 \rightarrow -1/2$   $GT$  transitions can be studied in the  $\beta$  decay of  $^{41}\text{Ti}$  to  $^{41}\text{Sc}$ . Two indepen-

dent  $\beta$ -decay measurements have been reported and the obtained  $B(GT)$  distributions were significantly different in the energy region above  $E_x=6$  MeV. If isospin is a good quantum number, the transition strengths of the  $T_z=\pm 3/2 \rightarrow \pm 1/2$   $GT$  mirror transitions should not be much different. It was found that the general feature of the  $B(GT)$  distribution deduced by Honkanen *et al.* [18] was similar to that observed in the present  $^{41}\text{K}(^3\text{He},t)$  measurement. In addition, the good energy resolution achieved by Honkanen *et al.* in the delayed proton measurement after the  $\beta$  decay was comparable with our resolution.

Through a detailed comparison of the  $T_z=\pm 3/2 \rightarrow \pm 1/2$   $GT$  transitions, one-to-one correspondences of analog states in  $^{41}\text{Ca}$  and  $^{41}\text{Sc}$  could be identified up to the excitation energy of 6 MeV, where the main transition strength was observed. In the identification, it was assumed that the strengths of the analogous transitions should be similar. The  $GT$  states in  $^{41}\text{Ca}$  and  $^{41}\text{Sc}$  can have a  $J^\pi$  value of either  $1/2^+$ ,  $3/2^+$ , or  $5/2^+$ , but the  $J^\pi$  assignment of individual states in  $^{41}\text{Ca}$  and  $^{41}\text{Sc}$  was not always clear. As a result of the identification of analog states, the most probable  $J^\pi$  values were assigned for each pair of analog states by combining the independent  $J^\pi$  information of the pair of corresponding states.

On the basis of the  $J^\pi$  assignment, the  $B(GT)$  strength distribution could be separately obtained for the three  $J^\pi$  values. It was found that the main part of the  $GT$  strength was carried by the  $5/2^+$  states. The gross features of the  $GT$  strength distributions for the three  $J$  states were similar for the isospin analogous  $T_z\pm 3/2 \rightarrow \pm 1/2$  transitions, but the details were somewhat different. From the difference of the distributions, isospin-asymmetry matrix elements of  $\approx 8$  keV were deduced. The difference of excitation energies was studied for analog states as a function of excitation energy. An energy increase of about 50 keV was observed at  $E_x=3.8$  MeV, suggesting a change of configuration in the wave function of the  $GT$  states below and above this energy.

The strengths of  $M1$  transitions in  $^{41}\text{Ca}$  from five excited states to the IAS were compared with the analogous  $GT$  transition strengths derived from the  $^{41}\text{K}(^3\text{He},t)^{41}\text{Ca}$  study. It was found that ratios of the  $M1$  and  $GT$  transition strengths, except for one transition, were similar. This suggests that the

contribution from the  $\ell\tau$  term, which is inherent to an  $M1$  transition and has no corresponding term in a GT transition, is small in these  $M1$  transitions.

#### ACKNOWLEDGMENTS

The  $^{41}\text{K}(^3\text{He}, t)^{41}\text{Ca}$  experiment was performed at RCNP, Osaka University, under the Experimental Program E195. The authors are grateful to the accelerator group of RCNP, especially to Professor T. Saito and Dr. S. Ninomiya, for

their effort in providing a high-quality and stable  $^3\text{He}$  beam indispensable for the realization of matching conditions required for achieving good energy and angular resolution. Y.F. thanks Professor J. Äystö (Jyväskylä, Finland) for valuable discussions and Dr. F.D. Smit (iThemba LABS, South Africa) for his comments in preparing the manuscript. This work was supported in part by Monbukagakusho, Japan, under Grant No. 15540274. B.A.B. acknowledges support from NSF Grant No. PHY-0244453.

- 
- [1] *Isospin in Nuclear Physics*, edited by D.H. Wilkinson (North-Holland, Amsterdam, 1969).
- [2] A. Bohr and B. Mottelson, *Nuclear Structure* (Benjamin, New York, 1969), Vol. 1, and references therein.
- [3] A. Bohr and B. Mottelson, *Nuclear Structure* (Benjamin, New York, 1975), Vol. 2, Chap. 6, and references therein.
- [4] F. Osterfeld, *Rev. Mod. Phys.* **64**, 491 (1992), and references therein.
- [5] J. Rapaport and E. Sugarbaker, *Annu. Rev. Nucl. Part. Sci.* **44**, 109 (1994).
- [6] T.N. Taddeucci, C.A. Goulding, T.A. Carey, R.C. Byrd, C.D. Goodman, C. Gaarde, J. Larsen, D. Horen, J. Rapaport, and E. Sugarbaker, *Nucl. Phys.* **A469**, 125 (1987), and references therein.
- [7] P.M. Endt, *Nucl. Phys.* **A521**, 1 (1990); **A633**, 1 (1998), and references therein.
- [8] Y. Fujita *et al.*, *Phys. Rev. C* **66**, 044313 (2002).
- [9] Y. Fujita *et al.*, *Phys. Rev. C* **59**, 90 (1999).
- [10] R. Madey, B.S. Flanders, B.D. Anderson, A.R. Baldwin, C. Lebo, J.W. Watson, S.M. Austin, A. Galonsky, B.H. Wildenthal, and C.C. Foster, *Phys. Rev. C* **35**, 2011 (1987); **36**, 1647 (1987).
- [11] Y. Fujita *et al.*, *Phys. Rev. C* **67**, 064312 (2003).
- [12] B.D. Anderson *et al.*, *Phys. Rev. C* **54**, 602 (1996).
- [13] B.A. Brown and B.H. Wildenthal, *At. Data Nucl. Data Tables* **33**, 347 (1985).
- [14] Y. Fujita *et al.*, *Eur. Phys. J. A* **13**, 411 (2002).
- [15] G. Audi and A.H. Wapstra, *Nucl. Phys.* **A565**, 1 (1993); **A595**, 409 (1995).
- [16] R.G. Sextro, R.A. Gough, and J. Cerny, *Phys. Rev. C* **8**, 258 (1973).
- [17] Z.Y. Zhou, E.C. Schloemer, M.D. Cable, M. Ahmed, J.E. Reiff, and J. Cerny, *Phys. Rev. C* **31**, 1941 (1985).
- [18] A. Honkanen, P. Dendooven, M. Huhta, G. Lhersonneau, P.O. Lipas, M. Oinonen, J.-M. Parmonen, H. Penttilä, K. Peräjärvi, T. Siiskonen, and J. Äystö, *Nucl. Phys.* **A621**, 689 (1997).
- [19] W. Liu *et al.*, *Phys. Rev. C* **58**, 2677 (1998).
- [20] Y. Fujita *et al.*, *Nucl. Phys.* **A687**, 311c (2001).
- [21] W.G. Love and M.A. Franey, *Phys. Rev. C* **24**, 1073 (1981).
- [22] M. Fujiwara *et al.*, *Nucl. Instrum. Methods Phys. Res. A* **422**, 484 (1999).
- [23] Y. Shimbara *et al.*, *Nucl. Instrum. Methods Phys. Res. A* **522**, 205 (2004).
- [24] T. Noro *et al.*, RCNP (Osaka University), Annual Report, 1991, p.177.
- [25] Y. Fujita, K. Hatanaka, G.P. A. Berg, K. Hosono, N. Matsuoka, S. Morinobu, T. Noro, M. Sato, K. Tamura, and H. Ueno, *Nucl. Instrum. Methods Phys. Res. B* **126**, 274 (1997), and references therein.
- [26] T. Wakasa *et al.*, *Nucl. Instrum. Methods Phys. Res. A* **482**, 79 (2002).
- [27] H. Fujita *et al.*, *Nucl. Instrum. Methods Phys. Res. A* **484**, 17 (2002).
- [28] Y. Fujita *et al.*, *J. Mass Spectrom. Soc. Jpn.* **48**, 306 (2000).
- [29] H. Fujita *et al.*, *Nucl. Instrum. Methods Phys. Res. A* **469**, 55 (2001).
- [30] J.A. Cameron and B. Singh, *Nucl. Data Sheets* **94**, 429 (2001), and references therein.
- [31] D.R. Tilley, H.R. Weller, and C.M. Cheves, *Nucl. Phys.* **A564**, 1 (1993).
- [32] C.D. Goodman, C.A. Goulding, M.B. Greenfield, J. Rapaport, D.E. Bainum, C.C. Foster, W.G. Love, and F. Petrovich, *Phys. Rev. Lett.* **44**, 1755 (1980).
- [33] W.G. Love, K. Nakayama, and M.A. Franey, *Phys. Rev. Lett.* **59**, 1401 (1987).
- [34] DW81, a DWBA computer code by J.R. Comfort (1981) and updated version (1986), an extended version of DWBA70 by R. Schaeffer and J. Raynal (1970).
- [35] T. Yamagata, H. Utsunomiya, M. Tanaka, S. Nakayama, N. Koori, A. Tamii, Y. Fujita, K. Katori, M. Inoue, M. Fujiwara, and H. Ogata, *Nucl. Phys.* **A589**, 425 (1995).
- [36] S.Y. van der Werf, S. Brandenburg, P. Grasdjik, W.A. Sterrenburg, M.N. Harakeh, M.B. Greenfield, B.A. Brown, and M. Fujiwara, *Nucl. Phys.* **A496**, 305 (1989).
- [37] R. Schaeffer, *Nucl. Phys.* **A164**, 145 (1971).
- [38] R.G.T. Zegers *et al.*, *Phys. Rev. Lett.* **90**, 202501 (2003); S.Y. van der Werf and R.G.T. Zegers (private communication).
- [39] H. Fujita, Ph.D. thesis, Osaka University, 2002 (unpublished); H. Fujita *et al.*, (unpublished).
- [40] E.K. Warburton, J.A. Becker, and B.A. Brown, *Phys. Rev. C* **41**, 1147 (1990).
- [41] B.A. Brown, A. Etchegoyen, and W.D.M. Rae, computer code OXBASH, MSU Cyclotron Laboratory Report No. 524, 1986.
- [42] A. Bohr and B. Mottelson, *Nuclear Structure* (Benjamin, New York, 1969), Vol. 1, illustrative example to Sec. 3-1.
- [43] N.I. Kaloskamis, A. García, S.E. Darden, E. Miller, W. Haerberli, P.A. Quin, B.P. Schwartz, E. Yacoub, and E.G. Adelberger, *Phys. Rev. C* **55**, 640 (1997).
- [44] A. García, E.G. Adelberger, P.V. Magnus, H.E. Swanson, D.P. Wells, F.E. Wietfeldt, O. Tengblad, and ISOLDE Collabora-

- tion, Phys. Rev. C **51**, R439 (1995).
- [45] J.A. Nolen and J.P. Schiffer, Annu. Rev. Nucl. Sci. **19**, 471 (1969).
- [46] N. Auerbach, Phys. Rep. **98**, 273 (1983).
- [47] Y. Fujita, B.A. Brown, H. Ejiri, K. Katori, S. Mizutori, and H. Ueno, Phys. Rev. C **62**, 044314 (2000), and references therein.
- [48] E.K. Warburton and J. Weneser, in *Isospin in Nuclear Physics*, edited by D.H. Wilkinson (North-Holland, Amsterdam, 1969), Chap. 5, and references therein.
- [49] S.S. Hanna, in *Isospin in Nuclear Physics*, edited by D.H. Wilkinson (North-Holland, Amsterdam, 1969), Chap. 12, and references therein.
- [50] H. Morinaga and T. Yamazaki, *In-Beam Gamma-Ray Spectroscopy* (North-Holland, Amsterdam, 1976), and references therein.
- [51] Y. Shimbara *et al.*, Eur. Phys. J. A **19**, 25 (2004).
- [52] Y. Fujita *et al.*, Phys. Rev. Lett. **92**, 062502 (2004).